8th ICAAR 1989 KYOTO 8th Internationl Conference on Alkali-Aggregate Reaction

ALKALI-AGGREGATE REACTION IN NEW BRUNSWICK, EASTERN CANADA —PETROGRAPHIC DIAGNOSIS OF THE DETERIORATION

Tetsuya Katayama and Toshiaki Futagawa

Cement/Concrete Technical Development Center, Sumitomo Cement Co.,Ltd.
585 Toyotomi, Funabashi, Japan 274

1. ABSTRACT

Petrographic examinations were made of deteriorated concretes, based on optical microscopy and SEM observations of internal textures, micro-XRD and EPM analyses of void-filling products, mercury intrusion porosimetry, DTA/TG measurements and chemical analyses of the mortar portions. It was found that reacted aggregates are predominantly pebbles of slate and siltstone which include cryptocrystalline to microcrystalline quartz in their matrix, and that similar slate contained in a local aggregate currently used in this region showed deleterious reactivity according to the ASTM C289 chemical test. Microscopic studies also revealed that alkalies are concentrated in both reaction rims within aggregates and gel-fillings in the concrete. It is believed that the major factor of the deterioration is alkali-aggregate reaction, though such processes as freezing and thawing and salt-attacks are strongly superimposed.

2. INTRODUCTION

Deterioration of concrete structures due to alkali-aggregate reaction in Eastern Canada was first noted in Nova Scotia (1,2), and subsequently in the neigboring province of New Brunswick (3). During the 7th international conference on AAR in Ottawa, 1986, a field trip was made to affected structures in New Brunswick (4) and the senior author visited the structures. They are mainly bridges built about 30-50 years ago that have recently been subjected to repeated repairs. In some structures symptoms of alkali-aggregate reaction, such as rimed aggregates and pattern crackings with prominent exudation of white efflorescent materials, were recognized in the field. However, at the same time, there was strong evidence of freezing and thawing, such as scaling, pop-outs and corner deterioration followed by carbonation. There was also the possibility of salt-attacks suggested by the collapse of overlay from steel reinceforments and rust-stained stalactites under the structures, were noted in some of structures.

In an attempt to determine the main factor of this complicated deterioration, samples of concrete collected by the senior author from seven structures were studied in the laboratory. Because the samples are only fragmentary, some being taken from the structure surface and others from concrete blocks that had been removed on previous repairs, they may not represent the general figure of each structure, but even though, studying them may be helpful in diagnosing alkali-reactivity of these concretes. Laboratory studies of the concrete include: petrographic examination to clarify the rock types of reacted aggregates and detect reaction products from concretes, SEM observation, micro-XRD and EPM analyses of the reaction products, chemical analysis, DTA/TG measurements and mercury intrusion microporosimetry of the mortar fraction, and ASTM chemical test of an example of the local aggregate. The results showed much evidence of alkali-aggregate reaction which will be discussed in this paper.

3. RESULTS AND DISCUSSION

3.1 Petrography of Coarse Aggregate

The coarse aggregate found from each structure is well rounded pebble, dominated in common by slate (near phyllite) and siltstone of Paleozoic age with minor amounts of sandstone, siliceous shale, quartzite, rhyolitic tuff and granite of miscellaneous origin (Table 1). Carbonate rocks were rarely found. Most of the slate and some of the siltstone and sandstone, show signs of reaction on the fracture surface in concrete. That is, a dark reaction rim, together with a white, broad rim just inside the former, is noted on the periphery of aggregate (Fig. 1). These rocks contain coarse to fine-grained clastic quartz but the reacted portion is confined to the fine-grained matrix, composed of mosaic aggregation of cryptocrystalline to microcrystalline quartz. On the polished section only a dark reaction rim is visible. Siliceous rocks, like quartzite and rhyolitic tuff, only have the dark reaction rim. Illitic mica and chlorite are abundantly contained in the fine-grained matrix of slate. Vermiculite, which has been noted in the reacted, argillaceous rocks in Nova Scotia (5, 6), was not recognized. The rock types most affected are common to those in Nova Scotia. Sand-grained fragments of sea shells and steel slag are occasionally contained in the concrete.

A local coarse aggregate currently used in this region has a similar lithology to that used in the deteriorated concrete. It largely consists of Paleozoic slate and siltstone which contain cryptocrystalline to microcrystalline quartz in their matrix. Only a few pebbles develop a weatherd rim with a rusty stain, but its appearance is quite different from the reaction rims found in the concrete. Chemical analysis shows that the slate is richer in K_2O, MgO and FeO than in siltstone, suggesting that K_2O is concentrated in illitic mica while MgO and FeO in chlorite.

3.2 ASTM Chemical Test of Aggregate

Potential reactivity of slate and siltstone selected from the local aggregate was tested according to ASTM C289 (Fig. 2). The slate fell into the deleterious field with Sc 100-120 mmol/l and Rc 60-70 mmol/l, while the siltstone was marginal. The values of the slate nearly correspond with those of common Japanese Paleo-Mesozoic cherts which consist of microcrystalline quartz (7). The potential reactivity of the slate can be explained by the presence of fine-grained quartz in their matrix, while the marginal reactivity of the siltstone may be due to the result of dilution of the reactivity by dominating clastic quartz that is less reactive. Opal was not found in these rocks but this mineral does not likely exist, because opal deposited before the Tertiary ages recrystallizes through chalcedony to stable quartz during diagenesis (8). The reactivity of slate and phyllite has been noted (1, 9, 10), and the cause of the reactivity is attributed to chalcedony and microcrystalline quartz contained in these rocks (11). This particular evidence seems to suggest the strong possibility that such type of rock is capable of alkali-aggregate reaction under certain conditions.

3.3 SEM Observation of Reaction Products

In the concrete, white gel-like deposits are found within reacted aggregetes and rarely in the air-voids. The morphology of these materials varies greatly in the SEM order of observations. The fracture surface of the dark reaction rim on the aggregate is generally smooth but is full of dessication cracks, indicating this part is composed of true gel material. Flaky crystals are sometimes embedded in this gel-rich layer. On the other hand, the white inner rim deposits occuring inside the dark reaction rim, are generally crystalline: they have a range of morphology from flaky to platy crystal habit to the rosette-like aggregation composed of platy crystals, together with sponge-like to filament-like materials of minor occurence. Most of the morphology hitherto reported (12, 13) can be seen in the deteriorated concrete from the same structure in this region. A qualitative EDX analysis indicated that alkalies, in particular K_2O, is concentrated in the rosette-type crystals on the aggregate (Fig. 3). White deposits on the aggregate may contain portlandite and some calcium carbonates, such as calcite and vaterite as shown by micro XRD and EPM analyses.

There are two distinct types of void-filling materials found in the mortar. One is a white spheric gel which fills a relatively large air-void, up to 3mm in diameter, close to the reacted aggregate, and the other is a small, white crystalline globule, up to 1mm across, composed of closely packed prismatic to bladed crystals. Macroscopically, some of the gels have a rimmed structure with varying transparencies. Under SEM observations they are usually mixtures of both amorphous and crystalline materials, such as flaky and rosette-like crystals. The crystalline phases found in the spheric gels have similar morphology and composition with those found in the white inner rim on the aggregate. These are alkali-silica gels which have derived from reacted aggregates and precipitated in the cavity of the concrete. On the other hand, coarsely crystalline material in the small globules is usually heaped but sometimes shows a hexagonal outline, and qualitative EDX analysis detected the presence of SO_3 in addition to CaO and Al_2O_3, so that this phase is most probably ettringite. The globules of this mineral are easily isolated when the mortar is crushed by a hammer.

3.4 EPMA Compositions of Gel Deposits

The white spheric gels from three structures were polished and then subjected to quantitative EPMA measurements (WDX mode: 15KV 10nA, counting time 5s for alkalies) to diagnose the alkali-reaction (Table 2). It was confirmed that the materials are alkali-silica gels, containing about 50% SiO_2 and up to 20% CaO with varying amounts of alkalies up to 11% of K_2O and 5% of Na_2O. The composition of these gels is not uniform due to concentric structures noted above, showing a gradient from the surface to the center. That is, in some specimens alkalies are enriched toward the center, whereas in others the reverse is true. Where the rosette-like crystals are concentrated, the amount of alkalies, especially K_2O, is high, while, where massive gel dominates, CaO is rich and K_2O poor. The total value of analysis tends to be low, suggesting the abundance of water in this phase. These results are in general agreement with those of previous researchers (12,13). The origin of alkalies concentrated in the rosette-type crystals was not ascertained in this study, but there is a strong possibility that K_2O has been leached from illitic mica that is contained abundantly in the reacted slate, as pointed out by Cole et al.(14) on their reacted siltstone aggregate in concrete.

3.5 Micro-XRD Analysis of Reaction Products

The void-filling materials from four structures were too small for ordinary powder X-ray diffraction analysis, and consequently they were analyzed by a PSPC X-ray diffractometer (micro-XRD: beam diameter 100 microns). This method directly identified the heaped crystal aggregations in the small globules as ettringite, and monosulphate was not found at all (Fig.4). Analyses also showed that some of the white rim deposit on the aggregate contain vaterite, calcite and portlandite, indicating that this is the carbonated rim. Because the carbonated rim around the aggregate can be formed not only by alkali-aggregate reaction but also by freezing and thawing and, in highly permeable or cracked concrete (15), the presence of this alone could not be a proof of alkali-aggregate reaction.

On the other hand, analysis of spheric gels in which potassium rich rosette-like crystals are concentrated, detected a weak 12 A reflection (13,14,16), along with a set of strong dehydrated 10 A phase reflections (Fig.4). According to Oberholster (16), the structure of the 12 A phase is very sentisive to changes in moisture content, and the basal spacing at 12 A is easily shifted to 11-9 A in moderately high temperature or vacuum during the examination. Shayan et al.(17) observed the contraction of the basal spacing to occur even at 50°C for 3 hours. Accordingly, the crystalline material in the spheric gels is in the process of dehydration after formation. A number of complex and discrete lines obtained from the material necessitates detailed crystallographic study to be made of these phases. Another sample of spheric gel, having a low value of total analysis, only showed a 12 A peak with infrated back ground between 5-9 A. In this case a small amount of the 12 A phase would have crystallized within the amorphous gel matrix in the air void, but the dehydration of this phase did not take place.

3.6 Chemical Analysis of the Mortar Fraction

The mortar fraction of each structure was analyzed, treated with 1:100 HCl to extract cement-derived components. The results, normarized to a fixed value of insoluble residue (50%), indicated that CaO in the mortar is constant at around 20% and SO_3 nearly constant in the range of 0.6-0.8% (Table 3). It is therefore assumed that the cement used had an averaging SO_3 content of 2.2%, indicating a normal composition in respect to SO_3. Accordingly, no enrichment in SO_3 from surrounding environment had occurred in these concretes. The large crystals of ettringite now concentrated in the air voids, therefore, may be a result of recrystallization of poorly crystalline primary ettringite in the original concrete through a dissolution process of cement paste along cracks and fissures that were formed later by alkali-aggregate reaction (18).

Total alkalies in the mortar ranged from 0.3-0.8%, but the small values of most specimens may reflect a leaching process due to surface weathering because none of concrete specimens were drilled cores. Water-soluble chlorine showed a high level of concentration, irrespective of the sample sources, suggesting that the chlorine has been either derived from aggregates used or contaminated by deicing salt extensively used in this region in winter. XRD analysis detected the presence of Friedel's salt, $C_3A \cdot CaCl_2 \cdot 10H_2O$, in the mortars containing more than 0.2% water-soluble chlorine. The result suggests the possibility of chloride-attacks occuring, and the field evidence of steel rusting followed by the collapse of overlay in some structures support this assumption.

3.7 Microporosimetry of the Mortar Fraction

The distribution of micropores in the mortar was measured using a mercury intrusion porosimeter (pore diameters 30 A to 300 microns). All specimens have distribution peaks below the range of 10^3 A, which is far smaller than the size of entrained air voids, suggesting that none of them were effectively air-entrained concretes (Fig.5). A vague correlation was noted between the results of this examination and the field diagnosis of deterioration. Mortar specimens, taken from structures showing evidence of freezing and thawing in the field, in addition to alkali-aggregate reaction, tend to be dominated by medium-sized capillary pores at around 10^3 A. This aspect was noted by Kamata (19) experimentally, who found that hardened cement pastes without entrained air voids but dominated by the capillary pores in the order of 10^2 to 10^3 A radii, are most susceptible to freezing and thawing. Careful interpretation should be made, however, in employing this method because pore-size distribution can be affected by the carbonation process (20), as well as by a water/cement ratio and hydration age of concrete. The results of DTA/TG measurements of the mortars showed that the degree of carbonation and the content of portlandite is not particularly different among samples (Table 3). Accordingly, this approach may be helpful in diagnosing freezing and thawing in concrete.

4. CONCLUSIONS

1. Alkali-aggregate reaction was observed in all structures in close association with freezing, thawing and chloride-attacks.

2. Typical reaction products such as rosette-like crystals and amorphous alkali-silica gel were most prominent evidence for diagnosing aggregate reaction.

3. The presence of cryptocrystalline to microcrystalline quartz in the reacted slate and siltstone aggregates, is indicative of alkali-aggregate reactivity in these samples of concrete.

5. ACKNOWLEDGEMENTS

The authors are grateful to Professor T.W.Bremner of University of New Brunswick and Mr.J.W.King of Department of Transportation, Province of New Brunswick, Canada, for kind suggestions which motivated them to make the study.

REFERENCES

(1) Duncan, M. A. G. and Swenson, E. G. The Professional Engineer in Nova Scotia, 10, 16-19, 1969.
(2) Duncan, M. A. G., Swenson, E. G., Gillott, J. E. and Foran, M. R., Cement and Concrete Research, 3, 55-69, 1973.
(3) Haines, G. H. unpublished thesis, 1975. cited in Rogers, C. and Worton, S. Alkali -Aggregate Reactions in Canada-A Bibliography, Ontario Ministry of Transportation Engineering Materials Office, Report EM 73, 26p, 1988.
(4) Bremner, T. W., 7th International Conference on Alkali-Aggregate Reaction - Post Conference Field Trip Guide, New Brunswick, Aug. 22-24, 2p. 1986
(5) Duncan, M. A. G., Gillott, J. E., and Swenson, E. G., Cement and Concrete Research, 3, 119-128, 1973.
(6) Gillott, J. E., Duncan, M. A. G., and Swenson, E. G. Cement and Concrete Research, 3, 521-535, 1973.
(7) Katayama, T. and Futagawa, T., Proceedings of the 8th International Conference on Alkali-Aggregate Reaction, Kyoto, Japan, 1989.
(8) Mizutani, S., Sedimentology, 15, 419-436, 1970.
(9) Swenson, E. G., ASTM Proceedings, 57, 1043-1056, 1957.
(10) Kammer, H. A. and Karlson, R. W., Journal of the American Concrete Institute, 37, 665-671, 1941.
(11) Kelly, T. M., Schuman, L. and Hornibrook, F. B., Journal of the American Concrete Institute, 44, 57-80, 1948.
(12) Regourd, M. and Hornain, H., Proceedings of the 7th International Conference on Alkali-Aggregate Reaction in Concrete, Ottawa, Canada, 1986, 375-380. (publ. 1987).
(13) Davies, G. and Oberholster, R. E., Proceedings of the 8th International Congress on the Chemistry of Cement, Rio de Janeiro, 5, 249-255, 1986.
(14) Cole, W. F., Lancucki, C. J. and Sandy, M. J., Cement and Concrete Research, 11, 443-454, 1981
(15) Nepper-Christensen, P., Personal Communication, November 1986.
(16) Oberholster, R. E., Poceedings of the 6th International Conference, Alkalis in Concrete, Copenhagen, June, 419-433, 1983.
(17) Shayan, A. and Lancucki, C. J., Proceedings of the 7th International Conference on Alkali-Aggregate Reaction in Concrete, Ottawa, Canada, 1986, 392-397. (publ. 1987).
(18) Jones, T. N. and Poole, A. B., Proceedings of the 7th International Conference on Alkali-Aggregate Reaction in Concrete, Ottawa, Canada, 1986, 446-450. (publ. 1987).
(19) Kamata, E., Cement and Concrete, 460, 28-34, Tokyo, 1985. (in Japanese)
(20) Kondo, R., Daimon, M. and Akiba, T., Proceedings of the 5th International Symposium on the Chemistry of Cement, Tokyo, 3, 402-409, 1968.

TABLE 1 LITHOLOGY OF COARSE AGGREGATES

ROCK TYPE	AGGREGATES IN CONCRETE (5-20mm)							LOCAL AGGREGATE		
	B-90	B-60	M-81	D-52	P-57	T-70	T-74	5-10	10-14	14-20mm
CONGLOMERATE							8			
SANDSTONE	6**	3**	8	5*	5	3**	14	8	10	9
SILTSTONE	33**	41**	23*	31**	27**	42**	36**	43	36	24
SLATE	29**	30**	15**	10**	9**	18**	4	23	25	31
SILICEOUS SHALE	5**	8**	5*	4	14**	4	16	8	6	5
LIMESTONE	2				1			3	6	13
PHYLLITE	3	1			4	2		5	6	2
SHALE HORNFELS			1	3	1	4		1	2	2
QUARTZITE	2	4	17*	9*	3	2	4			
METABASALT					6	1				1
GABBRO	1		1	1		4	3	1	1	
RHYOLITIC TUFF	4*	4	8*	16*	14*	6*	12	2	6	6
GNEISS	8		11	10	11			3	2	5
GRANITE	7	9	11	11	5	14	3	3		2

* ONLY DARK RIM VISIBLE
** DARK AND WHITE RIMS VISIBLE

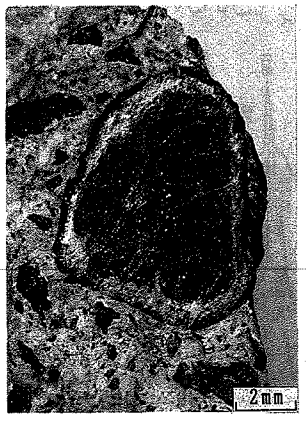

FIG. 1 REACTED SLATE WITH DARK OUTER RIM AND WHITE INNER RIM (M-81)

TABLE 2 EPMA COMPOSITIONS OF VOID-FILLING GEL

	T-70 (VOID A)		B-90 (VOID B)		P-57 (VOID C)	
	RIM	CORE	RIM	CORE	RIM	CORE
SiO_2	36.0 49.4	49.4 53.7	48.8 48.0	52.7 50.8	42.9 39.7	35.5 33.9
Al_2O_3	0.0 0.1	0.1 0.1	0.1 0.0	0.2 0.0	0.1 0.2	0.1 0.1
Fe_2O_3	0.0 0.0	0.0 0.0	0.1 0.0	0.1 0.0	0.0 0.1	0.0 0.0
CAO	19.5 22.4	14.6 20.7	19.5 18.1	12.9 12.2	20.8 22.0	24.5 27.3
MGO	0.0 0.0	0.0 0.2	0.0 0.1	0.0 0.0	0.0 0.0	0.0 0.4
Na_2O	0.3 0.4	1.0 1.2	3.3 2.6	4.6 5.2	4.4 0.7	1.1 1.6
K_2O	0.8 4.4	6.5 5.9	5.1 6.7	9.7 9.0	10.7 4.8	3.8 1.7
SO_3	0.0 0.0	0.0 0.0	0.0 0.0	0.0 0.0	- -	- -
TOTAL	56.6 76.7	71.6 81.8	76.9 75.5	80.2 77.2	78.9 67.5	65.0 65.0

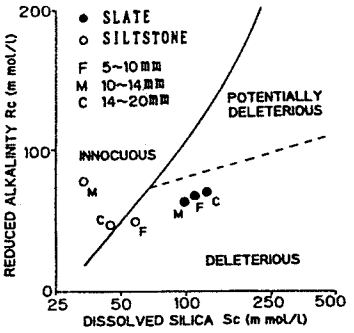

FIG. 2 ASTM C289 TEST OF THE SELECTED ROCK TYPES OF A LOCAL AGGREGATE

TABLE 3 ANALYSIS OF MORTAR FRACTION

	CAO[1]	Na_2O[1]	K_2O[1]	SO_3[1]	CL[2]	CAL[3]	POR[3]	ETT[4]	FRI[4]	POROSITY[5]
B-90	19.94	0.42	0.40	0.64	0.14	6.0	2.9	+		0.06
B-60	19.63	0.12	0.16	0.72	0.04	7.6	1.7	++		0.07
M-81	19.92	0.15	0.22	0.63	0.21	3.5	5.2	+	+	0.06
D-52	20.38	0.11	0.18	0.69	0.43	7.4	3.2	+	++	0.08
P-57	20.68	0.15	0.17	0.87	0.30	6.8	4.3	+	+	0.05
T-70	19.88	0.22	0.19	0.74	0.20	8.4	3.0	+	+	0.07
T-74	17.23	0.13	0.20	0.61	0.14	5.4	2.2	+		0.13

1) 1:100 HCL EXTRACTION NORMARIZED TO INSOLUBLE RESIDUE 50.0%
2) WATER-SOLUBLE CHLORINE
3) DTA/TG MEASUREMENT: CAL- CALCITE $CACO_3$, POR - PORTLANDITE $CA(OH)_2$
4) POWDER XRD ANALYSIS: ETT - ETTRINGITE $3CAO \cdot Al_2O_3 \cdot 3CASO_4 \cdot 32H_2O$
FRI - FRIEDEL'S SALT $3CAO \cdot Al_2O_3 \cdot CACL_2 \cdot 10H_2O$, + TRACE, ++ COMMON
5) MERCURY INTRUSION METHOD (cc/g)

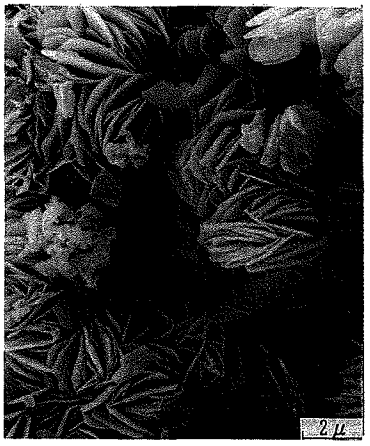

FIG. 3 ROSETTE-LIKE CRYSTALS IN THE WHITE INNER RIM DEPOSITS ON A REACTED SLATE AGGREGATE (B-90)

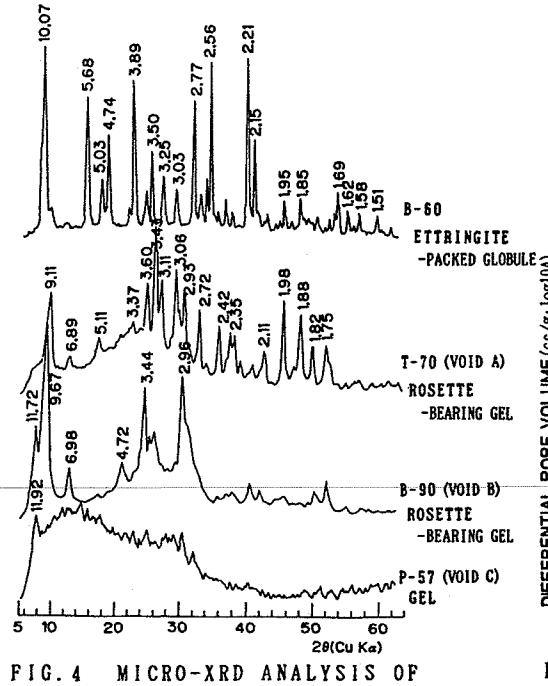

FIG. 4 MICRO-XRD ANALYSIS OF VOID-FILLING MATERIALS

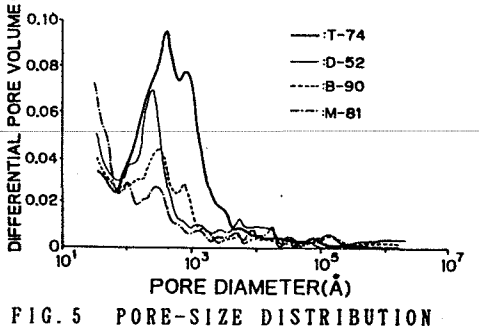

FIG. 5 PORE-SIZE DISTRIBUTION OF MORTAR FRACTION